Experimental comparison of Kalman and complementary filter for attitude estimation

G. Perez Paina, D. Gaydou, J. Redolfi, C. Paz, and L. Canali

Research Centre in Informatics for Engineering (CIII)
National Technological University, Córdoba Regional Faculty (UTN-FRC)
{gperez,dgaydou,jredolfi,cpaz,lcanali}@scdt.frc.utn.edu.ar
http://ciii.frc.utn.edu.ar

Abstract. This paper presents an experimental comparison of the Kalman and complementary filter for attitude estimation of a micro-uav quadrotor,fusing measurements from inertial MEMs devices. Simulations on Kalman and complementary filters are performed to study how the parameters affect the estimations of each one. Finally, the experimental results are presented using real data, which are used for both noise parameter modelling and comparing the performance of the filters given different operating conditions of the experimental plataform.

Keywords: Kalman filter, complementary filter, attitude estimation, quadrotor, UAV

1 Introduction

Spacecrafts, aircrafts, ships and many other vehicle's control systems rely on high quality states estimations to operate correctly. This also holds true for unmanned micro mobile robots. Good state estimations require, among other things, high precision inertial measurement devices. These kind of instruments are expensive and heavy, and that makes them unsuitable for unmanned micro robots applications. The advancements made on MEMS (Microelectromechanical systems) sensor technologies on the last years have produced low cost, small size, lightweight and acceptable performance inertial sensors. These characteristics make them suitable for low cost, portable and low power applications where rough (that means, to some extent noisy) measurements fullfill the requierements. The mentioned characteristics make these sensors atractive for unmanned micro vehicles like quadrotors. However, in this case the noise and bias level inherent to this technologies, as well as those produced by mechanical vibrations of the support structures leave these measurements beyond the accuracy necessary for the attitude stabilization compensators. This problem can be solved by means of fusion techniques like the Kalman filter or the complementary filter, which allow an acceptable estimation based on noisy and biased measurements from different sensors like accelerometers and gyroscopes. This work presents an experimental comparison for the tilt angle or "attitude" estimation, using two different sensor fusion techniques. This measurement estimation will be applied

in the control systems of a quadrotor type flying robot or UAV (Unmanned Aerial Vehicle). One of the fusion techniques to be studied is the Kalman filter, which is broadly used in state estimation, and the other technique is the complementary filter, used generally in applications of navigation using inertial sensors, fusing information of different sources. [1] shows the design of a low-cost and low-weight attitude estimation system based on the fusion of measurements from a gyroscope and an inclinometer using a complementary filter. The results are compared with the attitude value obtained with a potentiometer. Another one dimensional attitude system that implements the Kalman filter using measurements from an accelerometer and a low-cost gyroscope, is presented in [2]; even thought the sensor model applied is rather simple, the experimental results are satisfactory. A recent work [3], presents the implementation of a complementary filter in an embedded system for the attitude estimation using inertial sensors. Apropriate tests are performed for each sensor, accelerometer and gyroscope, to obtain the noise spectral characteristics of the measurements for different operating conditions. Applying a complementary filter to these signals yields satisfactory attitude estimations to stabilize the platform.

The paper is organized as follows. In section 2 and 3 the Kalman and the complementary filter design is performed. The results from the simulations appear in section 4, and section 5 shows the experimentals results. Conclusions are presented in section 6.

2 The Kalman filter

The Kalman filter calculates the best estimate of the state of a dynamic system from noisy measurements, minimizing the mean squared error of the estimate. It operates in two stages: *prediction* and *correction*, given the discrete stochastic equations describing the system dynamics.

$$x_{k+1} = Fx_k + Gu_k + w_k \tag{1}$$

$$z_k = Hx_k + v_k \tag{2}$$

where x is the system state vector, F is the state transition matrix, G is the control signals matrix gain and u is the input vector; z is the measurement vector, H relates the current state with the measurement, w is the process noise and v is the measurement noise.

Covariance matrices for w_k and v_k are

$$\mathbb{E}[w_k w_j^T] = \delta_{kj} Q_{kj}, \quad \mathbb{E}[v_k v_j^T] = \delta_{kj} R_{kj}, \quad \mathbb{E}[w_k v_j^T] = 0$$

For an optimal performance of the filter it is neccesary that noise sources are independent Gaussian processes with zero-mean [4, p. 94] and that the system dynamics is linear.

2.1 Measurement Model

Measurement errors can be divided into two main types, deterministic and stochastic. The deterministic part includes constant biases, scale factors, misalingments, axis nonorthogonality, which are reduce by calibration techniques. The stochastic part contains random error (noise) which cannot be removed and should be modeled as a stochastic process [5].

The most widely adopted model for gyro-accelerometer measurement systems, and also the chosen for the present work, is presented in [6]. This model assumes that the gyroscope measurements are affected by a constant drift or bias ω_b and a Gaussian white noise with zero mean n_ω. The derivative of the bias is a white noise with zero mean and Gaussian distribution n_α. It also assumes that the measurements of the accelerometer are affected by white noise with zero mean and Gaussian distribution n_θ

$$\dot{\theta} = \omega_M - \omega_b - n_\omega, \quad \dot{\omega}_b = n_\alpha, \quad \theta_M = \theta_T + n_\theta \tag{3}$$

In summary, the measurement models of the accelerometer and the gyroscope are presented in the eq. (4) [1]

$$\begin{aligned} \theta_M &= \theta_T + n_\theta, \quad & n_\theta &\sim \mathcal{N}(0, \sigma_\theta) \\ \omega_M &= \omega_T + \omega_I, & & \\ \omega_I &= \omega_b + n_\omega, \quad & n_\omega &\sim \mathcal{N}(0, \sigma_\omega) \\ \dot{\omega}_b &= n_\alpha, & n_\alpha &\sim \mathcal{N}(0, \sigma_\alpha) \end{aligned} \tag{4}$$

2.2 Estimation model for the angle

The Kalman filter equations ((1) and (2)) are use to estimate the angle θ, and the gyroscope bias ω_b. Assuming the gyroscope measurement as input signal and the accelerometer signal as the correction measurement

$$x = \begin{bmatrix} \theta & \omega_b \end{bmatrix}^T, \quad u = \omega_M, \quad z = \theta_M \tag{5}$$

The discrete state equations are

$$\begin{bmatrix} \theta_{k+1} \\ \omega_{b,k+1} \end{bmatrix} = \begin{bmatrix} 1 & -t_s \\ 0 & 1 \end{bmatrix} \begin{bmatrix} \theta_k \\ \omega_{b,k} \end{bmatrix} + \begin{bmatrix} t_s \\ 0 \end{bmatrix} \omega_{M,k} + t_s \begin{bmatrix} n_{\omega,k} \\ n_{\alpha,k} \end{bmatrix} \tag{6}$$

$$\theta_{M,k} = \begin{bmatrix} 1 & 0 \end{bmatrix} \begin{bmatrix} \theta_k \\ \omega_{b,k} \end{bmatrix} + n_{\theta,k} \tag{7}$$

where t_s is the sampling time, $\omega_{M,k}$ and $\theta_{M,k}$ are the kth measurement of the gyroscope and the accelerometer respectively. The process noise

$$w_k = t_s \begin{bmatrix} n_{\omega,k} \\ n_{\alpha,k} \end{bmatrix}, \quad Q = \mathbb{E}[w_k w_k^T] = t_s^2 \begin{bmatrix} \sigma_\omega^2 & \sigma_{\omega\alpha} \\ \sigma_{\omega\alpha} & \sigma_\alpha^2 \end{bmatrix} \tag{8}$$

[1] the subscript $_M$ indicates measured and subscript $_T$ represents true or real

and the measurement noise

$$v_k = n_{\theta,k}, \quad R = \mathbb{E}[v_k v_k^T] = \sigma_\theta^2 \tag{9}$$

The Kalman filter assumes that the process and the measurement noise are not correlated.

3 The complementary filter

The complementary filter is a simplified version of the Wiener filter, suitable for applications where the spectral description of the noise is not available [7].

3.1 Application to accelerometer and gyroscope measurements

Fig. 1 shows the block diagram of the complementary filter in continuous time, which also includes the transfer functions of both sensors. Here θ_a is the angle measured by the accelerometer whose signal is affected by high frequency noise. θ_g is the angle measured by the gyroscope affected by drift due to bias and is calculated as the integral of the measured angular velocity, ω_M. $\hat{\theta}$ is the estimated angle.

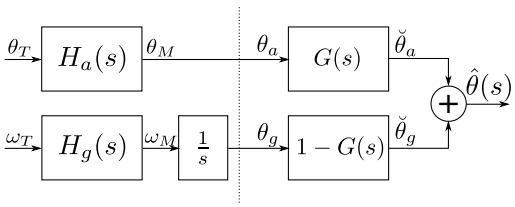

Fig. 1: Complementary Filter applied to accelerometer and gyroscope measurements

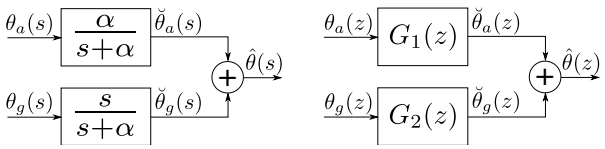

(a) continuous time (b) discrete time

Fig. 2: Complementary filter diagram

The filter transfer functions should be selected as $H_a(s)G(s) + H_g(s)(1 - G(s)) = 1$ where $H_a(s)$ and $H_g(s)$ represent the accelerometer and gyroscope transfer functions respectively. With this election, if the input signal is not affected by noise, the signal output is the same as the input. Assuming that the transfer functions of the sensors are equal to 1 ($H_a(s) = H_g(s) = 1$), the model of the filter is shown in Fig. 2a.

The transfer functions $G(s)$ and $1 - G(s)$ from Fig. 1 can be seen in Fig. 2a. These transfer functions show that the low frequency estimate depends on the accelerometer measurement removing the high frequency noise, and that the high frequency components of the estimate is dominated by the contribution of the gyro measurements, where the low frequency components of bias have been eliminated by the high-pass filter.

3.2 Discretization of the filters

In order to implement the digital filters, the transfer functions are discretized using the $\mathcal{Z}$ transform, assuming a zero order holder at the input, Fig. 2b. This gives a compact expression for the complete filter. The details of the discretization and the difference equations for the implementation can be seen in [3].

4 Simulation results

The parameters used in the simulation correspond to the listing 1.1.

Listing 1.1: Parameters used for simulation

```
t_s =  0.010000          ;[s]
nsteps =  1000
speed_bias =  10         ;[deg/s]
std_angle =  13          ;[deg]
std_speed =  40          ;[deg/s]
R =  0.051480
Q =  0.00005   0.00000
     0.00000   0.48739
fc =  0.50000            ;[Hz]
tau =  0.31831           ;[s]
```

Here t_s is the sampling interval, R and Q are the measure and process covariance matrices respectively; `fc` is the cut-off frequency of the complementary filter. Noisy signals with normal distribution and zero mean were generated, with the standard deviation values shown in listing 1.1 (`std_`). Also a constant bias value (`speed_bias`) was added to the gyroscope measurement.

4.1 Kalman Filter

Fig. 3 shows the estimation results of the Kalman filter, plotting the angle signal with noise, the true signal and the estimate. In this simulation the initial state of the angle $x_1 = \theta_{M,0}$ correspond to the first sampled value of the accelerometer, and the initial state of the bias $x_2 = \omega_b = 0$; it can be seen how the estimate is afected by the initial state.

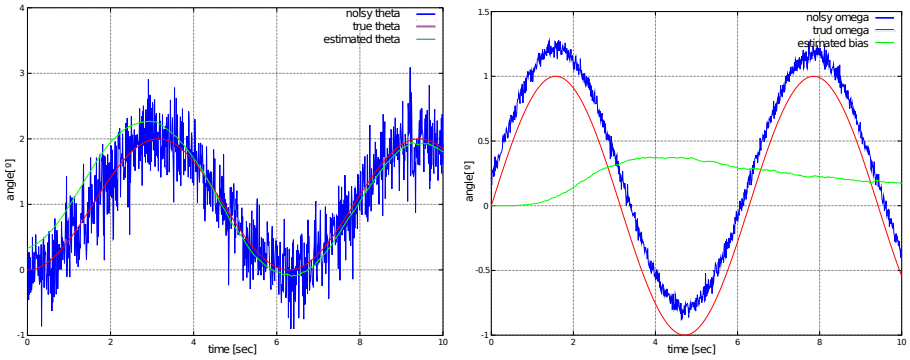

(a) angle estimation $\hat{\theta}$ (b) bias estimation $\hat{\omega}_b$

Fig. 3: Estimation using Kalman filter with $\mathbf{x_0} = [\theta_{M,1} \quad 0]^T$

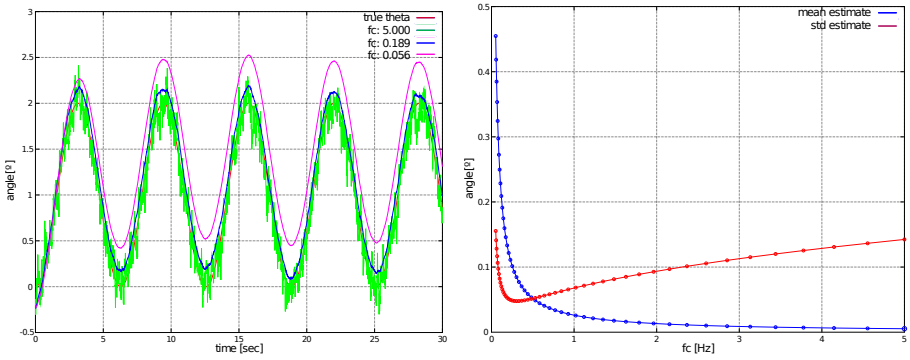

(a) estimated angle $\hat{\theta}$ (b) mean and standard value of the estimation error

Fig. 4: Estimation using the complementary filter for different values of f_c

4.2 Complementary filter

Fig. 4 shows the graphs of the results in the angle estimation using the complementary filter for different cut-off frequency values f_c. Fig. 4a shows the comparison between the estimated value and the true value; and Fig. 4b shows the mean and standard deviation of the estimation error.

Note that the mean of the estimation error decreases as the value of f_c decreases while the variance increases. That is, the estimation has less bias at the expense of a larger variance in the estimate. In Fig. 4b a minimun in the value of the variance can also be seen.

4.3 Comparison between Kalman and complementary filter

Fig. 5 shows the comparison between the Kalman and complementary filter estimation for different cut-off frequency values of the latter.

Listing 1.2 shows the mean value and the variance of the estimation error.

Listing 1.2: Mean and variance of the estimation error

```
mean_Kalman = -0.28950
var_Kalman =  0.54749
mean_comp =  2.2548
var_comp =  0.12696
```

5 Experimental results

The experimental comparison between the Kalman and complementary filter is performed using a testbed, which consists of a seesaw (rocker) [3] capable of emulating one of the rotational degree of freedom (roll or pitch) of a quadrotor. The platform consists of a movable bar attached to a base with bearings to reduce friction, which can rotate an angle of $\pm 40°$, see Fig. 6. It includes a low noise linear potentiometer to measure the angle of inclination, used as ground truth for comparison of the estimation results. On the opposite ends of the bar two separate engine-blade sets are mounted and the IMU (Inertial Measurement Unit) is attached to the middle.

The sensor used is a comercial IMU model 3DM-GD1 from Microstrain, built on a triaxial gyroscope, accelerometer and magnetometer. Raw measurements of the sensors were used for this work.

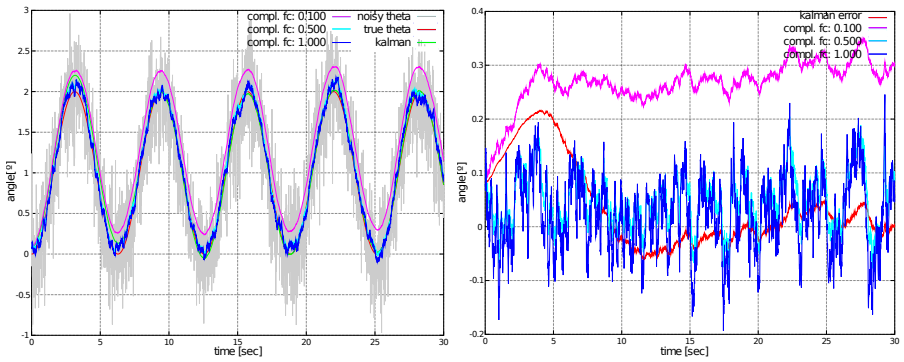

(a) (b)

Fig. 5: Comparison between Kalman and complementary filter for different values of f_c

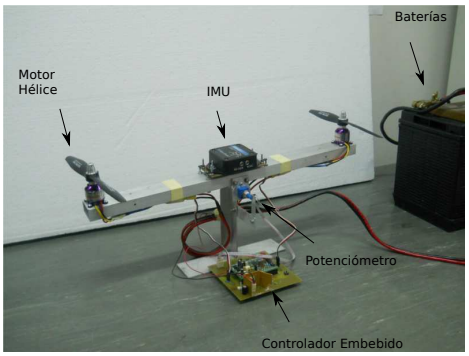

Fig. 6: Experimental platform

5.1 Sensors noise characterization

Adjusting the filter's parameter requires finding the covariance matrices of the measurements noise (R) and that of the process noise (Q) for the Kalman filter. On the other hand the cut-off frequency of the complementary filter must be determined. The best value fits the compromise solution of rejecting the low frequency noise on one sensor and also rejecting the high frequency interferences of the other [8].

To calculate the covariance matrices σ_θ, σ_ω and σ_α must be determined (Eq.(4)). Even thought these values are of great importance in the filter behavior, bibliography does not present any closed method to obtain Q and R. Some authors use manufacter's specifications [2], other apply some rough criteria for an initial aproximation and then perform a try-error cycle until satisfactoy behavior is achived. [9] presents an attempt to model Q and R but the tests show that the estimations diverge and heuristics corrections are again necessary.

The approach proposed in this work is to obtain σ_θ and σ_ω from statistical analysis of experimental data sets. σ_α is difficult to obtain from measurements, so it is adjusted experimentally based on the desired filter behavior. The measurements were taken with the rocker locked, avoiding angle changes but allowing the vibration to affect the sensors. The experiments were performed several times and sets of hundreds of thousands of samples were collected and processed to obtain $\sigma_\theta = 19.97$, $\sigma_\theta^2 = 398.62$, $\sigma_\omega = 2.96$ and $\sigma_\omega^2 = 8.75$.

Calculation of Q and R (Eq. (8) and Eq. (9)). The covariance matrix Q depends on processes' noise variance and on the sample time ($t_s = 0.01312s$) for the experiments. Since it is assumed that θ and ω are not correlated the covariance matrix Q is diagonal. The σ_α^2 setting process begins with a value less than σ_ω^2 and is trimmed to obtain the desired filter behavior.

$$Q = t_s^2 \begin{bmatrix} \sigma_\omega^2 & \sigma_{\omega\alpha} \\ \sigma_{\omega\alpha} & \sigma_\alpha^2 \end{bmatrix} = \begin{bmatrix} 1.505 \times 10^{-3} & 0 \\ 0 & 1.721 \times 10^{-4} \end{bmatrix} \tag{10}$$

The calculation of the covariance matrix of the measurement noise R is easier since it is a scalar.

$$R = \sigma_\theta^2 = 19.97^2 = 398.62 \tag{11}$$

5.2 Calculation of f_c

Fig. 7 shows the results obtained by sweeping f_c in the complementary filter. In Fig. 7b the mean and variance of the error depict a similar behavior as in the simulation (Fig. 4b). Because of the bias on measurements signals of the gyroscope; the input angle (θ_g) of the high-pass filter can be decomposed as an unbiassed part (θ_{gM}), plus a ramp function (θ_{gb}) product of the bias integral. (See fig. 1)

$$\theta_g = \theta_{gM} + \theta_{gb} \tag{12}$$

The output angle of the branch can be thought as the sum of the filtered signals

$$\breve{\theta}_g = \breve{\theta}_{gM} + \breve{\theta}_{gb} \tag{13}$$

Then the steady state value of $\breve{\theta}_{gb}(t)|_{t\to\infty}$ can be calculated as

$$\breve{\theta}_{gb}(t)|_{t\to\infty} = \lim_{s\to 0} s\frac{s}{s+\alpha}\frac{A}{s^2} = \frac{A}{\alpha} \quad ; \quad \alpha \sim f_c \tag{14}$$

which means that the steady state errors increases as the cut-off frequency decreases.

5.3 Experimental comparison between Kalman and complementary filter

Fig. 8 shows the experimental results obtained with the motors turned-off. The estimations of the filters are compared against the data aquired from the potentiometer, and this error shows a mean $\mu_{eK} = -0.96$ and a variance $\sigma_{eK}^2 = 3.4$ for the Kalman filter; while the error mean and the error variance are $\mu_{eC} = 0.12$ and $\sigma_{eC}^2 = 4.97$ respectively for the complementary filter. Transient data is not considered on these calculations.

Fig. 9 shows the estimations obtained from an experiment performed with the motors turned-on. The other conditions remain the same as the experiments of the previous paragraph. In this case $\mu_{eK} = 0.04$, $\sigma_{eK}^2 = 0.2$ for the Kalman filter and $\mu_{eC} = -0.11$, $\sigma_{eC} = 1.69$ for complementary filter.

6 Conclusions

Comparative studies were performed between Kalman filter and complementary filter techniques, intended to be applied to the estimation of attitude angles of a quadrotor. Inertial sensor used were MEMS accelerometer and gyroscope.

An experimental method to obtain covariance matrices Q and R yields satisfactory results in the case of the Kalman filter. For the complementary filter a

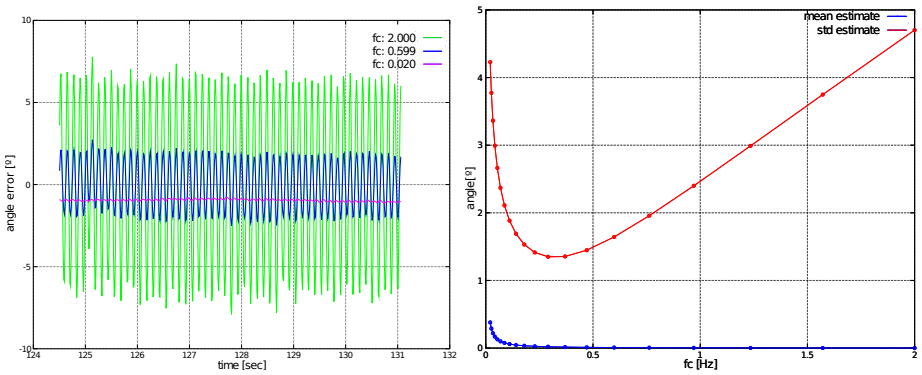

(a) temporal graphic (b) Mean and Variance estimation of error

Fig. 7: f_c sweep on complementary filter

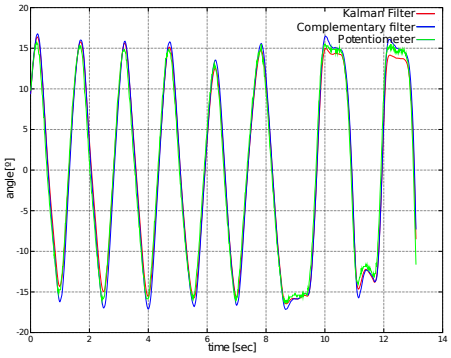

(a)

Fig. 8: Experimental comparison. Turned-off motors.

compromise choice for the cut-off frequency f_c affecting the mean and variance of estimation error was predicted in simulations and experimentally confirmed.

Finally the Kalman filter shows a noisier output than the complementary, but it is free of bias. This is convenient for applications were long term estimations are required. In the case of quadrotors the mission's time are not longer than 15 minutes, and with initial calibration the bias is not an issue for stabilization purpouses. As an advantage, the algorithmic simplicity makes the complementary filter the best choice for embedded applications, were not much computational power is available.

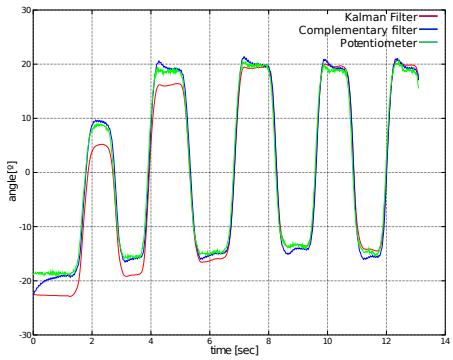

Fig. 9: Experimental comparison. Turned-on motors.

Acknowledgments

The two first authors are financed by the grants program "Becas de Formación de Doctores en Áreas Prioritarias. Ministerio de Ciencia, Tecnología e Innovación Productiva, Agencia Nacional de Promoción Cinentífica y Tecnológica - FONCyT IP-PRH 2007 - Resolución C.S. Nº 649/08

References

1. A.-J. Baerveldt and R. Klang. A low-cost and low-weight attitude estimation system for an autonomous helicopter. In *Intelligent Engineering Systems, 1997. INES '97. Proceedings., 1997 IEEE International Conference on*, pages 391 –395, sep 1997.
2. Young Soo Suh. Attitude estimation using low cost accelerometer and gyroscope. In *in AIAA 3rd Unmanned Unlimited Technical Conference, Workshop and Exhibit*, volume 2, pages 423–427, 2003.
3. D. Gaydou, J Redolfi, and A. Henze. Filtro complementario para estimación de actitud aplicado al controlador embebido de un cuatrirrotor. *CASE 2011, Congreso Argentino de Sistemas Embebidos*, 2011.
4. R.G. Brown and P. Hwang. *An Introduction to Random Signals and Applied Kalman Filtering*. John Wiley & Sons, third edition, 1997.
5. Petko Petkov and Tsonyo Slavov. Stochastic modeling of mems inertial sensors. *Cybernetics and Information Technologies*, 10(2), 2010.
6. Farrenkopf R. L. Analytic steady-state accuracy solutions for two common spacecraft attitude estimators. *AIAA Mechanics and Control of Flight Conference*, 1(4):282–284, 1978.
7. Yaakov Bar-Shalom, Thiagalingam Kirubarajan, and X.-Rong Li. *Estimation with Applications to Tracking and Navigation*. John Wiley & Sons, Inc., New York, NY, USA, 2002.
8. W.T. Higgins. A comparison of complementary and kalman filtering. *Aerospace and Electronic Systems, IEEE Transactions on*, AES-11(3):321 –325, May 1975.
9. E. Foxlin. Inertial head-tracker sensor fusion by a complementary separate-bias kalman filter. page 185, 1996.